Applied Catalysis A, General 558 (2018) 55–66

Contents lists available at ScienceDirect

Applied Catalysis A, General

journal homepage: www.elsevier.com/locate/apcata

Effect of CO_2 in the oxidative dehydrogenation reaction of propane over Cr/ZrO_2 catalysts

João F.S. de Oliveira[a], Diogo P. Volanti[b], José M.C. Bueno[a], Adriana P. Ferreira[a,*]

[a] DEQ - UFSCar, Rodovia Washington Luís, km 235, Jardim Guanabara, São Carlos, SP, Brazil
[b] IBILCE-UNESP, Rua Cristóvão Colombo, 2265, Jardim Nazareth, São José do Rio Preto, SP, Brazil

ARTICLE INFO

Keywords:
Chromium-zirconium oxides
Microwave
Oxidative dehydrogenation of propane
CO_2
Basic sites

ABSTRACT

Investigation was made on the effect of chromium content, and method of hydrothermal preparation of Cr/ZrO_2 catalysts on their catalytic properties for CO_2 oxidative dehydrogenation of propane (ODP). The catalysts were characterized by nitrogen physisorption, X-ray diffraction, Raman spectroscopy, and temperature programmed reduction and desorption of CO_2 (TPD-CO_2). The Cr/ZrO_2 catalysts containing various chromium contents between 2.5 and 15 wt.% of Cr were prepared by conventional and microwave-assisted hydrothermal methods. Tetragonal ZrO_2 was formed, with higher Cr contents, and smaller crystallite sizes obtained using the microwave-assisted method. The relationship between selectivity to propene and propane conversion suggested that independent of the preparation method, the catalytic properties could be classified in two groups, with low and high chromium contents. The TPD-CO_2 results showed that a fraction of the CO_2 was desorbed at temperatures higher than 500 °C, with simultaneous reduction of Cr(VI) species. The presence of CO_2 in the reactants caused strong decreases of activity, selectivity, and yield towards propene. These results suggested that CO_2 adsorbed strongly on the chromium oxide active sites for dehydrogenation of propane. The Cr/ZrO_2 catalysts were active and selective for dehydrogenation of propane in the absence of CO_2 (CDP), and became deactivated with time on stream. The activity was reestablished by thermal treatment with CO_2 or O_2 after deactivation in CDP catalytic cycles, with the activity always being reestablished by treatment in O_2. The deactivation occurred by reduction of Cr(VI) species and by deposition of carbonaceous species produced in oligomerization reactions.

1. Introduction

Propene is a major raw material for the petrochemical industry, being mainly used in polymer and rubber manufacture, and growth in the demand for it requires new production methods, since the two main commercial processes (steam cracking of naphtha or liquid petroleum gas, and fluid catalytic cracking of heavier oil fractions) have already reached their optima for propene production. Consequently, there has been intensive investigation of alternative routes with less energy expenditure, such as the transformation of alkanes to the corresponding alkenes, as well as other new technologies [1–3]. Selective dehydrogenation of propane to propylene is one of the major challenges for producing precious feedstocks [4]. An alternative route that has received attention recently is the non-oxidative catalytic dehydrogenation of propane (CDP) [1,5], which operates at high temperatures (above 800 K) in order to overcome thermodynamic constraints, with consequent catalyst deactivation due to propane/propene cracking and coke deposition [1,6], leading to decreased propene selectivity and yield. Commercial CDP catalysts contain supported CrO_x species as active components. For example, the CATOFIN and Snamprogetti processes utilize chromia-alumina catalysts in fixed and fluidized bed reactors, respectively [6]. Chromium oxide in the form of the Philips catalyst (Cr/SiO_2) presents moderate activity and olefin selectivity in the dehydrogenation of ethane and propane [7].

The oxidative dehydrogenation of propane (ODP) is attractive because the reaction is exothermic, and it can proceed at lower temperatures, suppressing coke formation [8,9]. It is accepted that the ODP reaction occurs according to the Mars-van Krevelen mechanism, which primarily consists of the cleavage of C—H bonds of the hydrocarbon (with the abstraction of hydrogen from the adsorbed alkane being described as the limiting step of the reaction), where the catalyst is reduced by the reaction between oxygen of the oxide network, and hydrogen abstracted from the hydrocarbon, forming water [9–12]. An in situ study at Cr K-edge XAFS spectra and TPR profiles demonstrates that the redox cycle between $Cr(III)O_6$ and $Cr(VI)O_4$ has an important pathway reaction in the dehydrogenation of C_3H_8 over both Cr/SiO_2, and Cr/Al_2O_3 catalysts [13]. Subsequently, there is the release of the olefin, and re-oxidation of the catalyst by the reactant mixture. This

* Corresponding author.
E-mail address: apf@ufscar.br (A.P. Ferreira).

https://doi.org/10.1016/j.apcata.2018.03.020
Received 15 December 2017; Received in revised form 19 March 2018; Accepted 20 March 2018
Available online 21 March 2018
0926-860X/

redox cycle should be able to maintain the stability of the catalyst over long periods of reaction [9–12]. Nevertheless, in the ODP reaction for industrially relevant alkane conversion, lower hydrocarbons and CO_2 are formed during successive oxidation of propene to carbon oxides [14], and unanswered questions remain concerning the factors governing the selectivity to propene [8,10,15]. There have been many studies of supported and unsupported catalysts based on metal oxides for the ODP. Among them, vanadium-based catalysts, especially highly dispersed VO_x species, have shown the best performances in terms of higher propane conversion, and propene selectivity [1,5,6,8,11,16,17]. Nevertheless, other metal oxides such as chromia (CrO_x) [18,19] have also been reported to deliver high performance in ODP, which has been ascribed to their high thermal, and mechanical stability, as well as relatively high surface area. Moreover, chromium supported on alumina, silica, or titania is known to be able to catalyze a range of important industrial reactions involving oxidation, polymerization, and hydrogenation-dehydrogenation. Chromium supported on zirconia has also been studied as a catalyst for the dehydrogenation of hydrocarbons and aromatization reactions [20–22], given the variability of its oxidation states [23–25]. However, these characteristics are strongly dependent on the amount of chromium, the treatment conditions, and the nature of the catalyst support [26–29].

The challenge remaining for technological advances in the ODP is related to the fact that this reaction favors complete oxidation of alkanes and olefins, so the viability of the process depends on the selectivity of the catalyst. In addition, the hydrocarbon/oxygen reactant mixture can be explosive, depending on the conditions used in the process. This drastically affects the olefins yield, due to the low concentrations of propane employed. In order to circumvent these problems and improve process selectivity and yield, carbon dioxide has been proposed as a mild oxidant to replace oxygen [2,29]. Technological advances, with increased propene yield, can be achieved using higher propane concentrations in the process and/or coke gasification by CO_2 [29,30]. Furthermore, CO_2 can shift the equilibrium to the product side and/or promote the dehydrogenation by means of reaction coupling between a simple dehydrogenation of propane and the reverse water-gas shift reaction [29,31,32].

Among the heterogeneous catalysts that have so far been studied for the ODP-CO_2 reaction, zeolites with MFI and CHA frameworks, including catalysts based on chromium [30,32–34], vanadium [10,34,35], and gallium [13,35,36], have been found to be the most effective materials, mainly due to their high activity and easy regeneration [37,38]. Metal oxide catalysts supported on MCM-41 have shown on-stream performance in the following order: Cr > > Ga > Ni > V > Fe > Mn > Co [34]. The use of a chromium catalyst in the reaction achieved three times higher propane conversion (around 17%) and propene yield (around 16%), compared to the performance of the second best metal catalyst [35]. Depending on the support, chromia-based catalysts employed in ODP using CO_2 have shown important differences, such as a negative effect of the partial pressure of CO_2 over chromium supported on alumina, since when CO_2 is strongly adsorbed on alumina, some of the carbon formed on the surface does not undergo reduction and the activity decreases. On the other hand, a positive effect of CO_2 has been found for samples of chromium supported on silica, attributed to the re-oxidation of Cr(III)/Cr(VI) species by CO_2 [13]. Wu et al. [36] reported that coke accumulation on the surfaces of chromium catalysts supported on zirconia decreased when ODP employed carbon dioxide. The hydrothermal synthesis of Cr/Zr catalysts has been reported to promote catalytic activity, due to greater amounts of polymeric Cr(VI) species, which have been associated with high catalytic activity in catalysts obtained using thermal treatments [36]. Although the use of CO_2 as an oxidizing agent in ODP reactions can potentially improve the process, the available literature data are not sufficient for any firm conclusions to be drawn. Promising results have been reported for Cr/ZrO_2 obtained by hydrothermal treatment, and here we propose catalyst preparation assisted by treatment in a microwave oven. This preparation method has recently been reported to be successful for the synthesis of oxides [37]. Due to the fast and homogeneous heating of the precursor solution, nucleation is faster, producing smaller crystallites and reducing the synthesis time [38]. The use of microwave heating was reported to lead to nanocatalysts with improved physical-chemical properties, compared to those fabricated by conventional methods, and a further attractive advantage lies in the possibility of performing nanocatalyst preparation using operationally simple one-pot methods based on “heating-up” techniques [38].

In the present work, evaluation was made of catalytic performance in the presence and absence of CO_2, using Cr/ZrO_2 catalysts obtained by conventional and microwave-assisted hydrothermal methods, addressing three main questions: (i) What is the effect of CO_2 on the performance of the Cr/ZrO_2 catalyst in the dehydrogenation of propane? (ii) What are the effects of the structural properties of Cr/ZrO_2 obtained by different methods and with different Cr contents on activity and selectivity? (iii) Is CO_2 effective in reactivation of Cr/ZrO_2 catalysts used in the ODP reaction?

Clarification of these issues is essential for the development of new high-yield processes for the dehydrogenation of propane.

2. Experimental

2.1. Catalysts synthesis

Cr/ZrO_2 samples were prepared by hydrothermal synthesis according to two methods: conventional and microwave-assisted. Aqueous solutions were prepared containing 0.25 M zirconium (IV) oxynitrate hydrate (Aldrich, 99%), and an amount of chromium (III) nitrate nonahydrate (Aldrich, 99%) resulting in samples containing 2.5, 5, 10, and 15 wt.% of Cr. Pure zirconia was prepared from an aqueous solution containing 0.25 M zirconium (IV) oxynitrate hydrate. The solutions were stirred vigorously at room temperature and an ammonia solution (6 M) was added dropwise until pH 10. After 1 h under stirring, the thermal treatments were applied. In the conventional method, autoclaves containing the solutions were heated at 180 °C in an oven, under a static atmosphere, for 24 h. In the microwave-assisted method, reactors containing the solutions were coupled to an adapted microwave oven and heated at 150 °C for 2.5 h (the maximum feasible temperature was lower than 180 °C in order to avoid increasing the internal pressure beyond safe limits). The precipitates from both thermal treatments were washed with distilled water, dried at 80 °C overnight, and calcined in air at 600 °C, increasing the temperature at 2 °C/min and maintaining the final temperature for 4 h. These catalysts were denoted x-yCZ, where x is the hydrothermal treatment used (c: conventional; m: microwave-assisted) and y is the chromium loading in the catalysts (2.5–15 wt. %). Commercial zirconia (Saint-Gobain) with tetragonal, and monoclinic phases were used as references.

2.2. Catalysts characterization

The digestion of samples was done using 10 mg of samples in an acid solution of HNO_3 (Aldrich, 70%), and HF (Aldrich, ≥48%), (2:1) heated at 90 °C during 30 min in a digest block. After that, the samples were diluted to 50 mL and Cr concentration was determined by inductively coupled plasma optical emission spectrometry (ICP-OES), using an Arcos spectrometer (Spectro).

Powder X-ray diffraction analyses (XRD) were performed using a Rigaku DMAX 2500 PC diffractometer operated at 40 kV and 150 mA, with Cu Kα radiation (λ = 1.5406 Å), Ni filter, 2θ from 10 to 70°, step size of 0.02°, and counting time of 2 s. The apparent crystallite sizes (D_{XRD}) of the ZrO_2 tetragonal phase (2θ = 30.3°) were determined using Scherrer’s equation [39,40].

Raman spectra of the materials were recorded using a Renishaw in spectrophotometer equipped with a solid state laser (633 nm wavelength, 17 mW capacity) as the excitation source and a 5x objective

lens. Spectra were collected at room temperature in the frequency range 200–1400 cm^{-1}.

Temperature-programmed reduction (TPR-H_2) profiles were recorded using an AutoChem II 2920 instrument (Micromeritics). Prior to the reduction, 45 mg of sample were pretreated at 150 °C for 1 h, under a flow of N_2 (White Martins 4.5 FID), followed by cooling to room temperature. TPR-H_2 was carried out by heating the sample from room temperature to 550 °C [41], at 10 °C min^{-1}, in 30 mL min^{-1} of 5% H_2 in He (White Martins 5.0 Analytical). H_2 consumption was measured using a thermal conductivity detector. The reduced samples were treated with CO_2 (White Martins, 99.9%) at 550 °C during 1 h, and a new TPR-H_2 experiment was performed to evaluate the CO_2 re-oxidation ability. The quantification of H_2 in TPR experiments was calculated by using a calibration curve obtained from CuO (Aldrich, 99.9%) as standard.

Temperature-programmed desorption of CO_2 (TPD-CO_2) profiles were obtained using the Micromeritics instrument (described above) coupled to a mass spectrometer (VaccumQuadstar 32, Pfeiffer). The as-prepared samples were pretreated for 1 h at 550 °C, under a flow of He (White Martins 5.0 Analytical). After cooling, the samples were saturated with CO_2 (White Martins, 99.9%) at room temperature, followed by heating from 50 to 1000 °C under a flow of He. TPD-CO_2 analysis of the previously reduced c-10CZ catalyst was also performed in order to determine the basic properties of the Cr sites.

Thermogravimetric analyses were performed using a thermobalance (Model SDT Q600, TA Instruments). After 300 min on stream, the used samples were heated to 1000 °C, at a rate of 10 °C min^{-1}, under a 30 mL min^{-1} flow of synthetic air (White Martins 5.0 FID). The carbon accumulation rate (r_c) was calculated using Eq. 1 reported in Supplementary material.

2.3. Catalytic performance tests

Activity measurements were carried out at atmospheric pressure, using a tubular fixed-bed quartz reactor (10 mm i.d.). The calcined catalyst (0.200 g) was deposited on quartz wool and heated from room temperature to 550 °C, under flow of 20 mL min^{-1} of He (White Martins 5.0 Analytical), for 1 h. The temperature was monitored using a thermocouple placed coaxially in the catalyst bed. The catalytic tests were performed using on-stream temperature-programmed reactions (TPSR) during a total time of 300 min. The reactant feed gas for the oxidative dehydrogenation of propane (ODP) was supplied at 20 mL min^{-1} and contained 2.5% (v/v) propane (Linde, 99.0%), 6.5% (v/v) CO_2 (White Martins 4.0), and the balance of He (White Martins 5.0 Analytical). For the catalytic dehydrogenation of propane (CDP), the reactant feed (supplied at 20 mL min^{-1}) consisted of 2.5% (v/v) propane and the balance of He. After 300 min on stream in the CDP reaction, the used catalysts were submitted to regeneration tests. For the used c-5CZ catalyst, 20 mL min^{-1} of synthetic air (White Martins 5.0 FID) was supplied for 5 min, or pure CO_2 (White Martins 5.0 Analytical) for 30 min, at 600 °C. For each catalytic cycle of 42 min on stream under the CDP reaction conditions, a regeneration procedure was applied, followed by a new catalytic cycle. The effluents were analyzed using a gas chromatograph (Model 7890 A, Agilent Technologies) equipped with a TCD detector and an HP-PLOT/Q capillary column. In all the tests, GHSV was kept at 0.5 min and the W/F ratio was 10 g min L^{-1}.

The values of propane conversion, CO_2 conversion, and selectivity to propene were calculated, respectively, according to Eqs. (2), (3), and (4) reported in Supplementary material.

The error of the conversions, and selectivity values are estimated by replications, and it is about 10% of each absolute value. The carbon balance was between 97 and 102%, calculated for each point of each test. Nevertheless, there is carbon accumulation at a low rate relative to reaction, and carbon is determined in used catalysts. The values of the CO/CO_2 mass balance and the hydrocarbons mass balance were calculated, respectively, according to Eqs. 5 and 6 reported in Supplementary material.

Table 1
Chemical analysis, structural characteristics obtained from XRD patterns, and ratio of Raman band intensities.

Catalyst	Nominal Cr/Zr wt.%	ICP analysis Cr/Zr wt.%	ZrO_2 phase	D_{XRD} (nm)	I_{1012}/I_{1034}
c-Z	–	–	Tetragonal and monoclinic	8.2	–
m-Z	–	–	Tetragonal	5.4	–
c-2.5CZ	2.5	3.6	Tetragonal and monoclinic	15.0	0.9
m-2.5CZ	2.5	3.5	Tetragonal	5.0	1.6
c-5CZ	5.0	7.5	Tetragonal	14.0	1.2
m-5CZ	5.0	7.5	Tetragonal	7.0	1.3
c-10CZ	10.0	13.5	Amorphous	n.d.	1.3
m-10CZ	10.0	12.0	Amorphous	n.d.	1.0
c-15CZ	15.0	18.2	Amorphous	n.d.	0.7
m-15CZ	15.0	19.6	Amorphous	n.d.	0.8

n.d.: not detected.

3. Results and discussion

3.1. Inductively coupled plasma optical emission spectrometry (ICP-OES)

Table 1 presents the Cr contents of the x-yCZ samples, determined using ICP-OES analysis. The samples synthesized by the conventional (c-) and microwave-assisted (m-) hydrothermal methods showed Cr contents higher than nominal, indicating lower yields of zirconia, relative to chromia, during the hydrothermal treatments.

3.2. X-ray diffraction (XRD)

Fig. 1 shows the XRD patterns of the commercial ZrO_2 phases (*m*: monoclinic; *t*: tetragonal) and the x-yCZ samples synthesized by the conventional and microwave-assisted hydrothermal methods and calcined at 600 °C. Table 1 summarizes the phases formed and the crystallite sizes of the x-yCZ samples. The diffraction peaks at 2θ of 30.3, 35.4, 50.0, and 60.0° were characteristic of the tetragonal ZrO_2 phase (JCPDS 50-1089), while peaks at 2θ of 24.2, 28.2, 31.4, 34.3, 41.5, 50.0, 53.0, 55.5, and 60.0° were characteristic of the monoclinic ZrO_2 phase (JCPDS 37-1484), as can be seen from the diffractograms for the commercial *m*-ZrO_2 and *t*-ZrO_2 samples. The diffractograms of the two ZrO_2 samples prepared in the absence of chromium (c-Z and m-Z) revealed that a mixture of tetragonal and monoclinic phases was formed in the sample synthesized by the conventional method (c-Z), while only the *t*-ZrO_2 phase was formed in the sample synthesized using the microwave method (m-Z).

The Cr-containing samples synthesized by the conventional method (Fig. 1A) showed a mixture of tetragonal and monoclinic ZrO_2 phases. Although the *t*-ZrO_2 phase predominated, both *t*-ZrO_2 and *m*-ZrO_2 were suppressed with increasing Cr content. For the Cr-containing samples synthesized by the microwave method (Fig. 1B), the main crystalline phase was *t*-ZrO_2. The samples with low Cr contents obtained by the microwave method showed lower degrees of crystallization, compared to the catalysts obtained by the conventional method. Table 1 presents the apparent ZrO_2 crystallite sizes for the as-prepared x-yCZ samples with various Cr contents, showing the smaller ZrO_2 crystallite sizes for the samples obtained using the microwave method. Considering that acceleration of the nucleation/crystallization process was expected in the microwave-assisted method, the smaller ZrO_2 crystallites obtained using this method could have been due rate of the nucleation is favored relative to rate of the crystallization due lower temperature of the treatment. Previous studies have shown that the presence and concentration of ions other than Zr ions can affect the crystallization of zirconia [19]. Hence, the degree of crystallization, which depends on the Cr content, indicates the dispersion of Cr in the precipitate formed. The samples obtained using the conventional method and with Cr

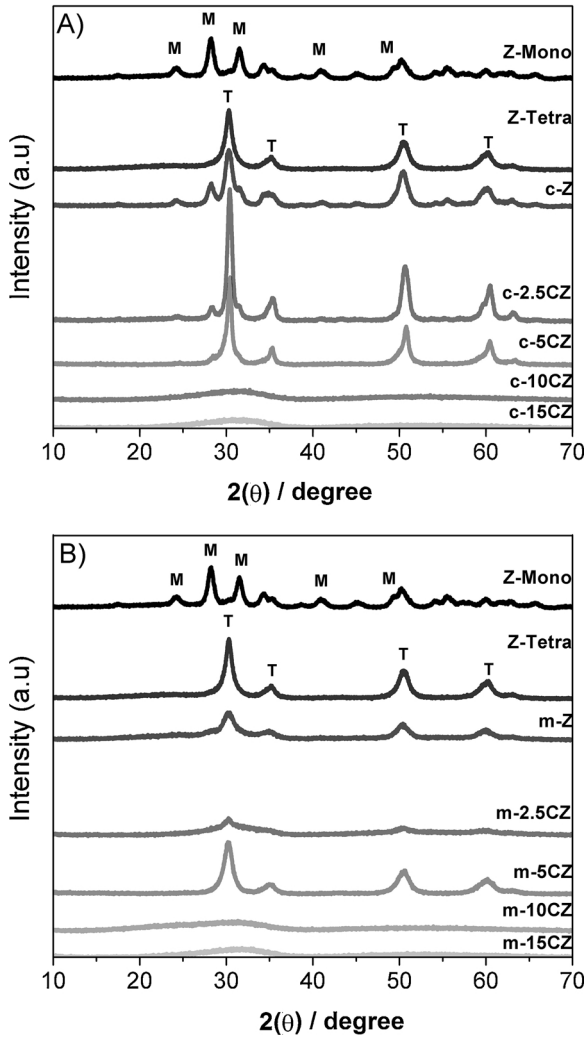

Fig. 1. XRD patterns of the calcined commercial *m*-ZrO_2 and *t*-ZrO_2, and of the calcined x-yCZ samples (x = hydrothermal synthesis method: conventional (c-) or microwave-assisted (m-); y = Cr wt.%).

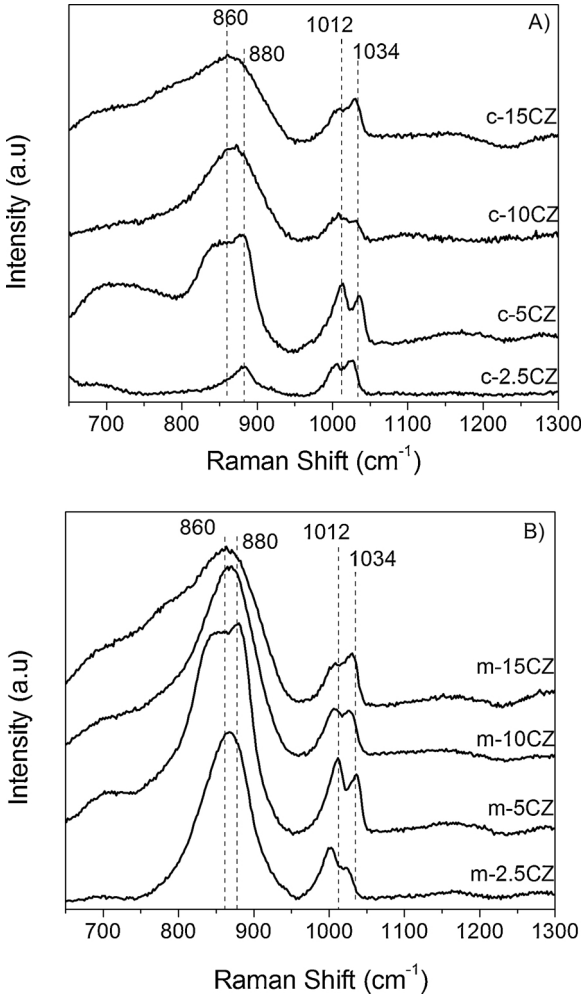

Fig. 2. Raman spectra of the calcined x-yCZ samples (x = hydrothermal synthesis method: conventional (c-) or microwave-assisted (m-); y = Cr wt.%).

contents of 2.5 and 5 wt.% showed higher degrees of crystallization, relative to pure ZrO_2. For the samples obtained using the microwave method and with low Cr contents, the crystallization of *t*-ZrO_2 was not linearly proportional to the Cr content, and the degree of crystallization of *t*-ZrO_2 was higher for 5 wt.% of Cr than for the sample containing 2.5 wt.% of Cr (Fig. 1B). The amorphous ZrO_2 phase was observed in samples containing over 10 wt.% of Cr (considering the Cr contents determined in the ICP analyses), obtained by both methods, indicating that the presence of greater amounts of chromium ions critically affected the structural organization of the zirconia. The characteristic peaks of α-Cr_2O_3 (at 2θ of 24.8, 32.8, 38.0, and 54.6°; JCPDS 01-0622) or metallic Cr (at 2θ of 24.2, 28.2, 31.4, 34.3, 41.5, 50.0, 53.0, 55.5, and 60.0°; JCPDS 37-1484) were not detected, suggesting that the chromia was highly dispersed on the ZrO_2.

3.3. Raman spectroscopy analyses

The Raman spectroscopy results for the calcined samples synthesized using the different hydrothermal methods revealed bands at around 860, 1012, and 1034 cm^{-1} (Fig. 2). The band at 1034 cm^{-1} could be attributed to vibration of terminal Cr = O of monochromate, while the bands at 1012 and 860 cm^{-1} were assigned to the terminal Cr═O and Cr−O−Cr bridge vibrations of polychromate, respectively [27,42]. The Raman spectra indicated the presence of both monomeric and polymeric surface Cr(VI) species in both the c-yCZ and the m-yCZ catalyst series. Table 1 presents the I_{1012}/I_{1034} band ratios for the as-prepared c-yCZ and m-yCZ samples. With the exception of the m-10CZ samples, the microwave-assisted method resulted in catalysts with higher I_{1012}/I_{1034} ratios, compared to the corresponding conventional catalysts, indicative of higher concentrations of surface Cr(VI) polychromate species, relative to monochromate species [43]. Wu et al. [36] associated higher I_{1012}/I_{1034} ratios with a greater predominance of polymeric Cr(VI) species, which are more easily reduced and re-oxidized, compared to monomeric Cr(VI) species [35].

For the m-yCZ sample series, the I_{1012}/I_{1034} ratio increased with decreasing Cr content. The same trend was not easily observed for the c-yCZ sample series, where the higher degree of crystallization was likely to have affected the type of chromium species formed. Although the formation of polychromate species was expected to be favored with increasing Cr contents, the experimental results showed the opposite. Considering that different ZrO_2 phases were formed for both x-yCZ catalyst series, depending on the Cr content, it is reasonable to infer that interaction of the chromium species depended on the ZrO_2 phase and the thermal treatment conditions. For example, the band at about 1034 cm^{-1} associated with monochromate species shifted slightly to a lower wavenumber for the samples containing highly amorphous ZrO_2 (m-2.5CZ, m-10CZ, and m-15CZ), obtained by the microwave-assisted method. On the other hand, the band at about 860 cm^{-1}, associated with polychromate species, shifted to higher wavenumbers for the samples containing highly crystalline ZrO_2 (c-2.5CZ, c-5CZ, and m-

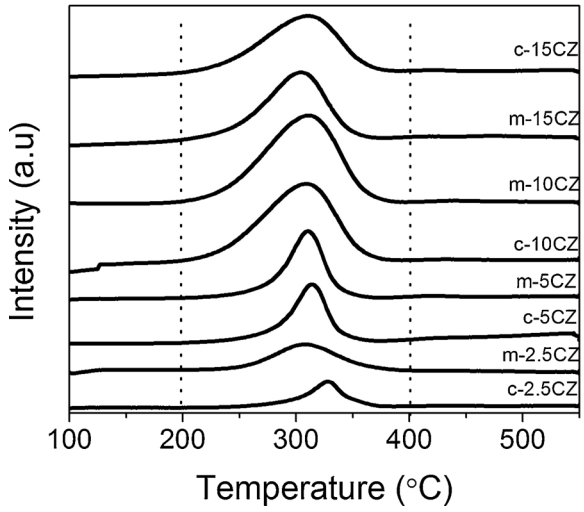

Fig. 3. TPR-H_2 of the calcined x-yCZ samples (x = hydrothermal synthesis method: conventional (c-) or microwave-assisted (m-); y = Cr wt.%).

5CZ). Notable differences were observed in the Raman band intensities at 860 cm^{-1} (assigned to the Cr-O-Cr bridge vibrations of polychromate) of the x-yCZ samples, depending on the preparation method. Higher intensities of this band were found for the samples obtained using the microwave-assisted method, compared to the conventional method. For example, considering samples with similar Cr contents, the intensity this band was about 6 times higher for m-2.5CZ than for the c-2.5CZ sample.

The presence of the broad band around 633 nm-excited spectra is due to photoluminescence (PL), and not Raman scattering of the samples, since Raman shifts appear at the same position, regardless the excitation wavelength [44]. Furthermore, the broadening of Raman band is also due to phonon contribution [45,46]. It is expected that nanostructured materials (the broad XRD patterns shown in Fig. 1 indicate the presence of nanomaterials) influence on the phonon Raman spectra, and the asymmetric broaden peak appear in the spectrum [47,48].

3.4. Temperature-programmed reduction analyses (TPR-H_2)

Fig. 3 shows the TPR-H_2 profiles of the x-yCZ samples. In all cases, a single reduction peak was observed, with a maximum in the temperature range 305–327 °C, which could be attributed to the reduction of Cr (VI) chromium oxide species to Cr(III) [24,27]. The reduction of Cr^{6+} ions to Cr^{3+} ions could occur according to a reaction of the following type: $Cr^{6+} + 3/2H_2 + 3HO^- \rightarrow Cr^{3+} + 3H_2O$ [7]. The intensity and width of the peaks increased with increasing Cr content, indicating changes of Cr(VI) species with Cr content. There was a slight displacement of the temperature for maximum H_2 uptake to lower reduction temperatures, as the chromium content increased. The highest reduction temperature was observed for the c-2.5CZ sample, reflecting higher interaction of the chromium oxides with ZrO_2. This sample showed the presence of *m*-ZrO_2 and *t*-ZrO_2 in well crystallized phases (Fig. 1A), together with a notable shift in the Raman spectrum (Fig. 2A). In comparison with the materials obtained using the conventional hydrothermal treatment, the results for the samples obtained using the microwave-assisted method (especially the m-CZ series containing chromium at up to 5 wt.%, as shown in Table 2) indicated that the polymeric Cr(VI) species present at higher concentrations in these samples were more easily reduced than monomeric Cr(VI) [25], as indicated by the Raman spectroscopy data (Table 1).

Table 2 presents the quantitative H_2 uptake data obtained from the TPR-H_2 profiles of the x-yCZ catalysts before and after re-oxidation by CO_2. The calcined samples were submitted to TPR-H_2 analysis and the amounts of Cr(VI) species present were calculated from the H_2 uptake. The reduced samples were then treated with CO_2 and a new TPR-H_2 analysis was performed in order to determine the quantity of chromium species that had been re-oxidized by CO_2. The percentages of Cr(VI) relative to total Cr in the calcined samples showed that the prevalence of the chromium (VI) oxidation state in the samples was dependent on the total Cr content. With the exception of sample m-2.5CZ, the amount of Cr(VI) increased with the total Cr content, with the maximum amount obtained for the samples containing about 10 wt.% of chromium (for both series of CZ samples). On the other hand, the data for the conventional CZ samples suggested the preferential formation of chromium (III) species, with the percentages of Cr(VI) relative to the total amount of Cr being lower than 50% (except for the c-10CZ sample). In addition, 15 wt.% of chromium in the samples seemed to be a critical Cr content that led to lower formation of Cr(VI) species, relative to other Cr species, regardless of the sample preparation method. As discussed before, the presence of a higher amount of chromium ions critically affected the structural organization of the zirconia. The c- and m-15CZ samples (which also contained amorphous structures, as shown in Fig. 1) did not contain similar small zirconia crystallites as the 10 wt.% samples, resulting in lower Cr(VI) formation. The Cr(VI) species formed in the c- and m-15CZ samples were preferentially monomeric, as shown by the Raman spectra (Fig. 2, Table 1), indicating that higher Cr contents led to particular characteristics of the materials.

Table 2
Quantification of Cr(VI) species from TPR-H_2 profiles before and after treatment of the x-yCZ samples with CO_2 (x = hydrothermal synthesis method: conventional (c-) or microwave (m-); y = Cr wt.%).

Catalyst	T_{max} (°C)	Cr(VI) (mmols/g_{cat}) in the as-prepared samples, and fraction of Cr(VI) ()[a]	Cr(VI) (mmols/g_{cat}) in the samples re-oxidized by CO_2, and fraction of Cr(VI) ()[b]
c-2.5CZ	327	0.31 (0.45)	0.10 (0.34)
m-2.5CZ	307	0.48 (0.71)	0.08 (0.14)
c-5CZ	314	0.67 (0.46)	0.13 (0.19)
m-5CZ	309	0.72 (0.50)	0.15 (0.21)
c-10CZ	307	1.72 (0.66)	0.29 (0.17)
m-10CZ	310	1.71 (0.74)	0.26 (0.15)
c-15CZ	310	1.23 (0.35)	0.07 (0.06)
m-15CZ	305	1.07 (0.28)	0.22 (0.21)

[a] Fraction of Cr(VI) relative to the amount of Cr in the as-calcined samples, based on ICP analysis.

[b] Fraction of re-oxidized Cr(VI) relative to the previous amount of Cr(VI) in the freshly calcined samples.

Table 2 also presents the H_2 uptake results for the samples reduced in H_2 and re-oxidized with CO_2, showing that only a fraction of the Cr (VI) species present in the as-calcined samples was available in the second reduction cycle. These results suggested that CO_2 did not provide efficient re-oxidation of chromia, as reported by Wu et al. [36].

3.5. Temperature-programmed CO_2 desorption analyses (TPD-CO_2)

Fig. 4 presents the TPD-CO_2 results for the zirconias (y-Z) and the x-yCZ catalysts, obtained using mass spectrometry monitoring of CO_2 at *m/z* 44. The pure zirconia obtained by both the conventional (c-Z) and microwave (m-Z) methods presented the main CO_2 desorption peaks at low temperatures in the range 100–300 °C, characteristic of weak basic sites [49], while the c-Z zirconia exhibited a small fraction of CO_2 desorbing at about 380 °C, characteristic of strong basic sites. Both pure zirconias showed *t*-ZrO_2 as the main crystalline phase (Fig. 1, Table 1), while the x-yCZ samples exhibited a mixture of *m*-ZrO_2 and *t*-ZrO_2 phases. Higher basicity is expected for the *m*-ZrO_2 phase, relative to the *t*-ZrO_2 phase, due to the lability and mobility of oxygen in the monoclinic structure [50]. The Cr-containing samples showed CO_2 desorption peaks at low temperatures in the range 100-200 °C, as well as at high temperatures in the range 500–700 °C. The first peak decreased

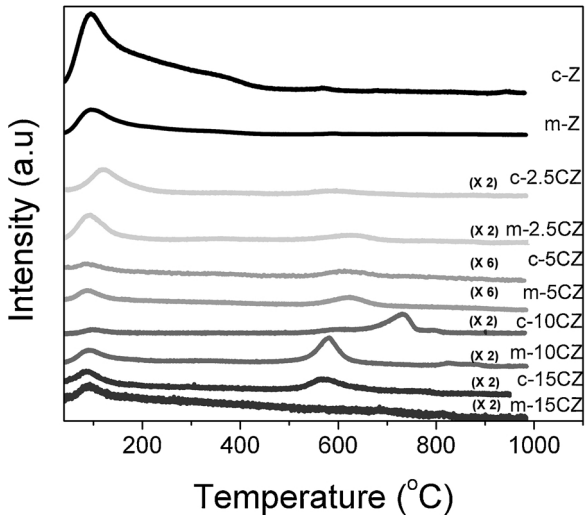

Fig. 4. MS signal for CO_2 during TPD-CO_2 of the as-prepared x-yCZ samples (x = hydrothermal synthesis method: conventional (c-) or microwave-assisted (m-); y = Cr wt.%). Factors within parentheses indicate the values by which the curve signal was multiplied in order to improve visualization.

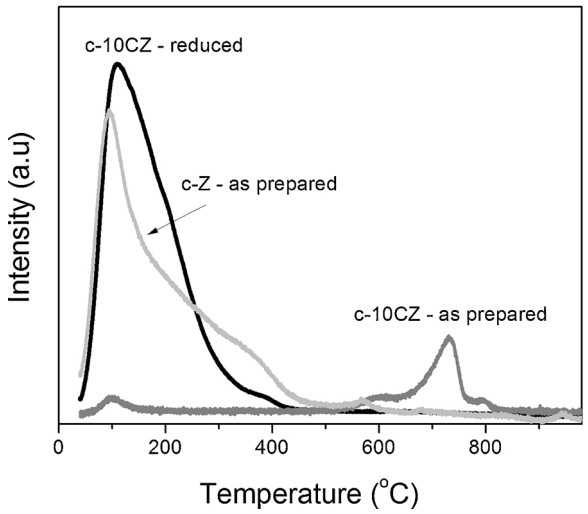

Fig. 5. MS signal for CO_2 during TPD-CO_2 of the c-10CZ catalyst, as-prepared and previously reduced in H_2.

with the Cr content. The temperature and intensity of the second peak were dependent on the Cr content and the catalyst preparation method, but were not directly correlated with the ZrO_2 phase. Considering that high basicity is not expected in amorphous and tetragonal ZrO_2 [50], the strong basic sites observed could have been formed by the interaction of different species of chromium oxide with ZrO_2. High intensity peaks were present at around 580 °C for the m-10CZ and c-15CZ samples and at a higher temperature of around 730 °C for the c-10CZ sample. The catalysts with chromium contents lower than 10 wt.% showed low intensity desorption peaks at around 630 °C. This population of sites desorbing CO_2 at high temperatures was not observed for the m-15CZ sample. Therefore, in order to investigate the basic properties of the sites according to the presence of Cr(III) or Cr(VI), TPD-CO_2 was performed with the c-10CZ sample, as-prepared and after reduction in H_2. The results are presented in Fig. 5. When the c-10CZ sample was reduced, the fraction of stronger basic sites from the as-prepared c-10CZ were replaced by a greater quantity of weaker basic sites, exhibiting a profile similar to that observed for the as-prepared zirconia without Cr (c-Z), with desorption of CO_2 at low temperatures. These results suggested that the Cr(VI) species in the x-yCZ samples interacted with

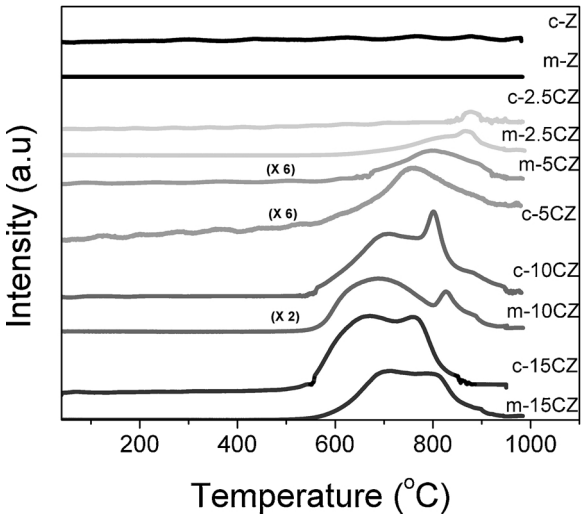

Fig. 6. MS signal for O_2 during TPD-CO_2 of the as-prepared x-yCZ samples (x = hydrothermal synthesis method: conventional (c-) or microwave-assisted (m-); y = Cr wt.%). Factors within parentheses indicate the values by which the curve signal was multiplied in order to improve visualization.

weak basic sites of Zr-O-Zr, resulting in strong basic sites of the type Cr (VI)-O-Zr, while Cr(III)-O-Zr resulted in weak basic sites.

Fig. 6 presents the results of TPD-CO_2 with monitoring of O_2 at *m/z* 32. Comparison of the profiles for CO_2 (Fig. 4) and O_2 (Fig. 6) showed that CO_2 and O_2 were formed and desorbed in similar temperature regions. Carbonate species could be formed by reaction of CO_2 with strong basic sites, which blocked these basic sites, while at high temperatures (550–950 °C) there was thermal reduction of Cr_2O_6 to Cr_2O_3 and desorption of O_2 [51].

3.6. Catalytic tests

Fig. 7 and Table 3 present the CDP and ODP-CO_2 catalytic results for the conventional and microwave-assisted CZ catalyst series, plotted in Fig. 7A and B, respectively. Propane conversion in the CPD reaction decreased strongly with time on stream, and this decrease during 300 min on stream is presented as the deactivation rate (ΔX_0 CDP) in Table 3. The fastest deactivations were observed for the samples with low chromium contents (Fig. 7), reflecting the reduction of Cr(VI) species in the samples with lower Cr(VI) contents (Table 2). Previous studies have demonstrated that Cr(VI) species promote the activity for CDP reactions, where propane is adsorbed in the first step [35,36,52]. The Cr(VI) species are not stable under dehydrogenation conditions, becoming reduced to Cr(III) with time on stream. The Cr(III) then becomes the active species, with lower activity for the dehydrogenation of light alkanes [12,29,35,36,53].

The initial propane conversion under CDP was higher than under ODP-CO_2 reaction conditions, for both the conventional and the microwave-assisted CZ catalyst series with different chromium contents (X_0 C_3H_8 CDP and X_0 C_3H_8 ODP; Table 3). The difference between the initial propane conversions in the two reactions was around 30% for some samples (especially the c- and m-10CZ catalysts). The initial CO_2 conversion under ODP-CO_2 reaction conditions (X_0 CO_2; Table 3) reaches around 50–60% of respective initial propane conversions for practically all samples, indicating that pathway reaction occur via CO_2 oxidation of Cr sites, but it is not an exclusive pathway. Besides, CO_2 conversions are always higher for microwave-assisted CZ catalyst series than conventional ones. The samples obtained by the microwave-assisted method provided higher initial propane conversions in the presence of CO_2, compared to the corresponding conventional samples, with these differences decreasing for the initial propane conversions under CDP (in the absence of CO_2). It is probable that CO_2 was absorbed

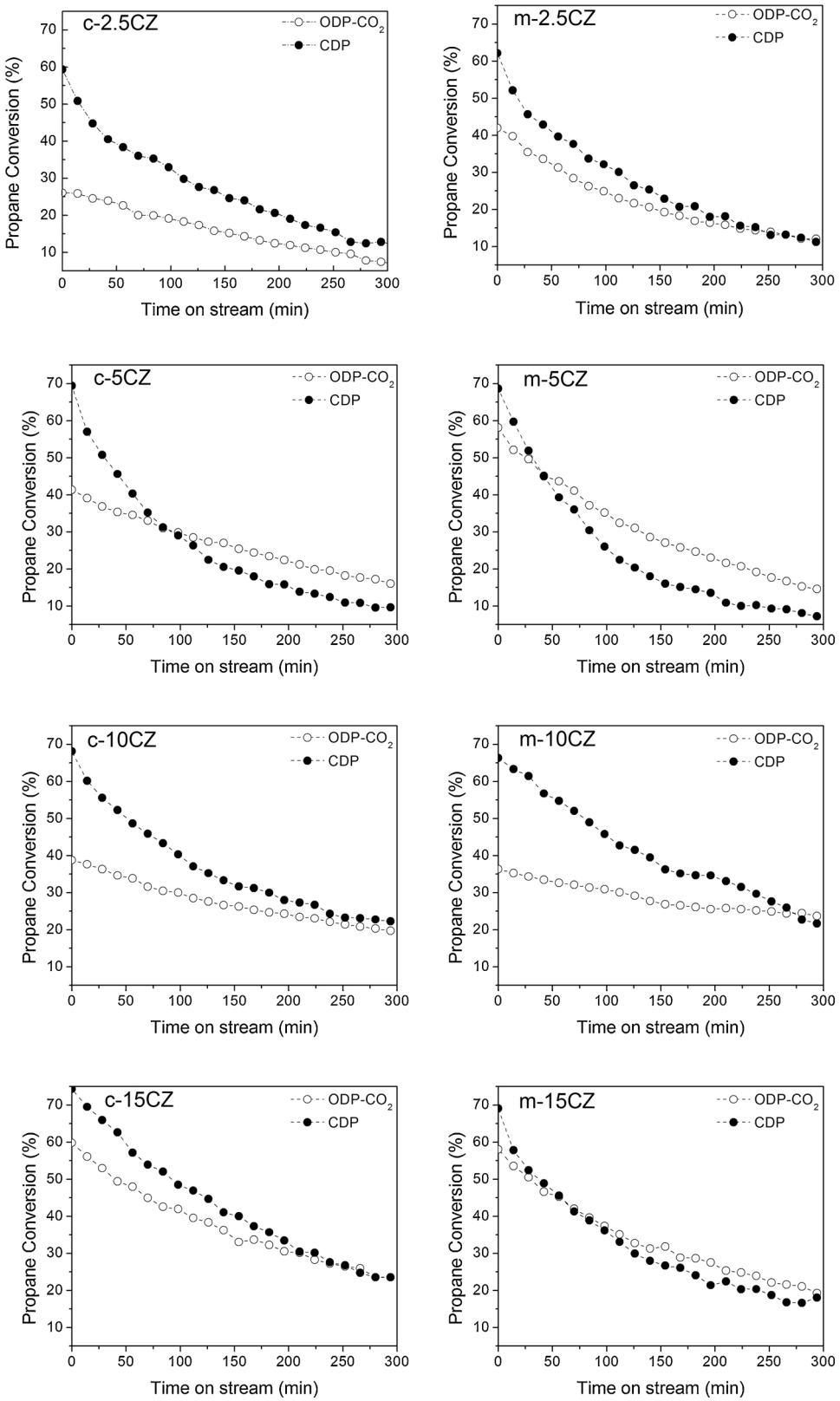

Fig. 7. Propane conversion as a function of reaction time under CDP and ODP-CO_2 reaction conditions at 550 °C for the as-prepared x-yCZ samples (x = hydrothermal synthesis method: conventional (c-) or microwave-assisted (m-); y = Cr wt.%). GHSV was kept equal to 0.5 min and the W/F ratio was 10 g min/L for all tests. The error of the conversion values is estimated at about 10% of each absolute value.

on the x-yCZ catalyst surfaces and/or on the Cr active sites, forming carbonate species at low temperatures and blocking the sites for propane adsorption in the first step. The TPD-CO_2 profiles confirmed the adsorption of CO_2 on weaker and stronger basic sites of the x-yCZ catalysts, with desorption of CO_2 as a function of temperature (Fig. 4). Although nanoparticles of oxides, with basic properties could be active for dehydrogenation of hydrocarbon at low temperatures, the strong adsorption of olefin on active site make the reaction impracticable at

Table 3
Initial C_3H_8 conversions (X_0), Initial CO_2 conversions (X_0 CO_2), initial specific activities ($r_{(CDP)0}$ and $r_{(ODP)0}$), initial propene yields (Y_0), and deactivation rates (ΔX_0) during the CDP and ODP-CO_2 reactions for the catalysts synthesized by conventional (c-) or microwave-assisted (m)methods.

As-prepared catalyst	X_0 C_3H_8 CDP (%)	$r_{(CDP)0}$ (% / mg_{Cr})[a]	X_0 C_3H_8 ODP (%)	$r_{(ODP)0}$ (% / mg_{Cr})[a]	X_0 CO_2 ODP (%)	ΔX_0 (% / g_{Cr}.min)[c]		Propene yield (Y_0, %)	
						CDP	ODP	CDP	ODP
c-2.5CZ	59	16.4	26	7.2	13 (8)[b]	0.21	0.10	47	18
m-2.5CZ	62	17.7	42	12.0	23 (11)[b]	0.19	0.09	50	25
c-5CZ	69	9.2	41	5.5	24 (13)[b]	0.13	0.06	51	26
m-5CZ	69	9.2	58	7.7	42 (14)[b]	0.15	0.10	45	30
c-10CZ	69	5.1	38	2.8	17 (12)[b]	0.06	0.02	54	26
m-10CZ	66	5.5	36	3.0	21 (10)[b]	0.06	0.01	50	25
c-15CZ	74	4.1	59	3.2	33 (17)[b]	0.05	0.03	57	34
m-15CZ	69	3.5	58	3.0	35 (15)[b]	0.04	0.03	45	34

Initial catalytic data (conversions, specific activities, and yields) refer to reaction times of 5 min in the CDP and ODP reactions.
[a] Specific activities calculated as the initial propane conversion/mg Cr, considering the Cr content from ICP analysis.
[b] CO_2 conversions after 300 min on stream.
[c] Deactivation rates calculated from the difference between the initial and final propane conversions in the CDP and ODP reactions, considering the Cr content from ICP analysis and 300 min on stream.

low temperature [54]. For ODP-CO_2 the strong adsorption of H_2O formed during oxidation could adsorb on active site [13]. Thus, reactants and products in ODP-CO_2 contribute to blocks the basic active site at low temperatures. Both effects caused decreases in the initial conversions in the presence of CO_2, independent of the zirconia structure, the preparation method, and the Cr content. The decrease of propane conversion during 300 min on stream is also presented in Table 3 as the deactivation rate (ΔX_0). All the catalysts became deactivated with time on stream at 550 °C. In both CPD and ODP-CO_2 reactions, propane conversion decreased strongly with time on stream, with the deactivation rates being higher in CDP than in ODP-CO_2. Consequently, for almost all the x-yCZ catalysts, the propane conversion curves intersected each other during the time on stream (Fig. 7), suggesting greater stability under ODP-CO_2 conditions. A redox process based on the Mars-van Krevelen mechanism [9,10] was expected to occur with these catalysts, improving their stability and propene selectivity [36]. This possibility was evaluated by TPR-H_2 analyses of the x-yCZ catalysts after their reduction and treatment with CO_2. The results (Table 2) revealed inefficiency of the x-yCZ catalysts in terms of re-oxidation of the Cr sites. However, the results demonstrated that all the Cr/ZrO_2 samples were partially re-oxidized by CO_2, even in low degrees, suggesting that the CO_2 adsorbed at strong basic sites participated in the catalytic cycle at high temperatures, with re-oxidation of chromium species. The reactivation of Cr(III) by CO_2 has been reported previously for Cr/SiO_2 catalysts [13].

The specific activities of the x-yCZ catalysts at the start of the CDP and ODP-CO_2 reactions decreased progressively with increasing Cr content of the samples (see $r_{(CDP)0}$ and $r_{(ODP)0}$ in Table 3), independent of the preparation method. The most active x-yCZ catalysts had the lowest Cr contents ($x \leq 5$ wt.%) and also presented the highest deactivation rates (ΔX_0). These results indicated that neither the zirconia phase nor the crystallite sizes could be individually responsible for formation of the active Cr species and/or their stability on stream. On the other hand, the Raman spectra (Fig. 2, Table 1) were indicative of correlation between the catalytic activity and a predominance of polymeric Cr(VI) species, relative to monomeric species, in the yCZ samples with lowest Cr contents. As mentioned before, the samples with lower Cr(VI) contents showed fast deactivation during time on stream, due to the reduction of Cr(VI) species (Table 2).

Both catalysts containing 5 wt.% of chromium (c- and m-5CZ) presented clear deactivation in the CDP reaction during the first 2 h on stream, with high slopes of the conversion curves. Consequently, the curves for propane conversion in the CPD and ODP-CO_2 reactions intersected each other much faster than for the other catalysts, with reversal of the activities during the time on stream (Fig. 7A and B). Interestingly, the c- and m-5CZ catalysts presented the pure tetragonal zirconia phase, with around 50% of Cr(VI) species, relative to the total Cr content (Table 2), and a predominance of polymeric Cr(VI) species, relative to the monomeric form (Table 1). The c- and m-5CZ catalysts also presented highly discreet populations of strong basic sites at the reaction temperature (Fig. 4). As discussed before for the TPD-CO_2 results (Figs. 4–6), the Cr(VI) species in the x-yCZ samples interacted with the weak basic Zr-O-Zr sites, resulting in strong basic sites of the type Cr (VI)-O-Zr, while Cr(III)-O-Zr resulted in weak basic sites, since high basicity is not expected in amorphous and tetragonal ZrO_2 [50]. Comparison of the profiles for CO_2 (Fig. 4) and O_2 (Fig. 6) showed that the CO_2 and O_2 were formed and desorbed in a similar temperature region (above 550 °C) corresponding to the reaction temperature for the c- and m-5CZ catalysts. Desorption of O_2 above 550 °C resulted from the decomposition of carbonate species and thermal reduction of Cr_2O_6 to Cr_2O_3, with the latter becoming the active species with lower activity for the dehydrogenation of light alkanes [12,29,35,36,53] and being responsible for the catalytic behavior in the CDP reaction. This analysis seems reasonable, because the m-2.5CZ catalyst presented practically the same structural and basic properties as the c- and m-5CZ catalysts, but showed a lower deactivation rate during the first 2 h in the CDP reaction. The m-2.5CZ catalyst only showed O_2 desorption at temperatures higher than 600 °C, avoiding the fast deactivation of the active Cr species observed for the c- and m-5CZ catalysts. The catalysts with Cr contents higher than 5 wt.% showed much greater O_2 desorption above 550 °C, but lower slopes of the conversion lines for the first 2 h in the CDP reaction. It could be concluded that the strongly basic Cr (VI)-O-Zr sites in the ZrO_2 crystalline structures were more active and less stable due to the higher lability and mobility of oxygen in the crystalline structure than in the amorphous ZrO_2 structure, which improve the basicity. Therefore, the large amounts of O_2 desorbed at 550 °C for the catalysts with Cr contents higher than 5 wt.% could have been derived from the decomposition of large quantities of carbonate species formed on a greater number of Cr sites.

Notably, the intersection between the curves of propane conversion in CDP and ODP-CO_2, followed by the inversion of the activities during the time on stream, occurred more rapidly for the microwave-assisted CZ catalysts than for the corresponding conventional catalysts (Fig. 7A and B), for all Cr contents. This indicated that the microwave-assisted hydrothermal method was able to form more active sites of chromium species, as could also be seen from the initial specific activities of the microwave-yCZ catalysts (Table 3). As shown in Fig. 8, the average rates of carbon accumulation on the m-yCZ catalysts during the time under ODP conditions were higher than on the c-yCZ catalysts with lower chromium contents ($y \leq 5$ wt.%). This was supported by the

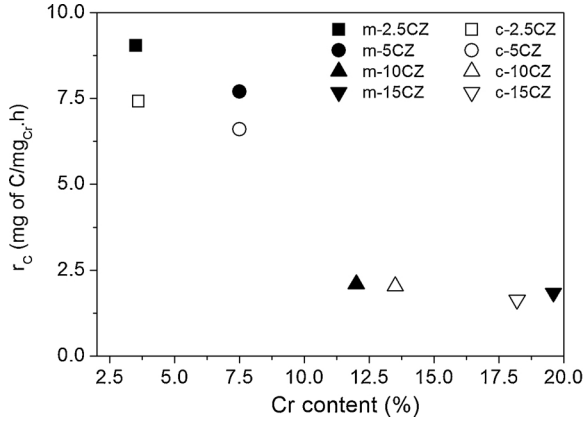

Fig. 8. Average carbon accumulation rates for the x-yCZ samples (x = hydrothermal synthesis method: conventional (c-) or microwave-assisted (m-); y = Cr wt.%), after 210 min on stream in the ODP-CO_2 reaction at 550 °C.

Raman spectra (Fig. 2), since the Raman band intensities at 860 cm^{-1} (assigned to Cr—O—Cr bridge vibrations of polychromate) of the x-yCZ samples were much higher for the samples obtained using the microwave-assisted hydrothermal method than for those obtained by the conventional hydrothermal method. The higher specific activities of the microwave-yCZ catalysts resulted in faster deactivation by the thermal reduction of Cr_2O_6 to Cr_2O_3, because the active Cr(VI) species were not stable under the reactions conditions and the mechanism of Cr(III) re-oxidation by CO_2 was inefficient (Table 2).

Fig. 9A and B show the selectivities to propene for the propane conversions in the CDP and ODP-CO_2 reactions, for the conventional and microwave-assisted CZ catalyst series, respectively. All the catalysts became deactivated and showed altered selectivity to propene with time on stream at 550 °C. In the CDP reactions, the decreased propane conversions were followed by increased selectivity to propene. In the low propane conversion region, the selectivity to propene was 100%. There was a maximum conversion value at which the selectivity to propene was 100%, after which the selectivity decreased as the conversion increased. This conversion maximum increased with the chromium content. For example, in the CDP reactions, 100% selectivity was achieved at propane conversions of 35 and 17% for the catalysts with 15% (c-15CZ) and 2.5% (c-2.5CZ) of chromium, respectively. Hence, the selectivity increased as the chromium content increased. The same behavior was observed in the ODP reactions, with the average rate of carbon accumulation on the x-yCZ catalysts during the time under ODP conditions decreasing with increase of the chromium content (Fig. 8).

In the CDP reaction, the initial propane conversion values at 550 °C exceeded 59% (Table 3), while the thermodynamic conversion for dehydrogenation of propane under these conditions is about 30% [55]. However, hydrogen was not detected among the products (Table 4), while the TPR results (Fig. 3) demonstrated that the x-yCZ samples were reduced by H_2 at a temperature of around 350 °C, which was lower than the reaction temperature. These results were indicative of a decrease of chromium oxides with time on stream, with higher propane conversion occurring by coupling of the propane dehydrogenation reaction ($C_3H_{8(g)} \rightleftarrows C_3H_{6(g)} + H_{2(g)}$) and the oxidation of H_2 by the chromium oxides, hence shifting the equilibrium. The similar initial propane conversion values for the catalysts with different chromium contents suggested that the initial reactions (X_0 CPD) were in quasi-equilibrium. However, the initial selectivities (Table 4) showed the formation of CH_4, C_2H_4, C_2H_6 and C_3H_4, which could be produced by oligomerization at acid sites [1], in addition to C_3H_6 formation. The presence of acid sites on the zirconia surface is known [45,56]. C_2H_4 and C_2H_6 are precursors of coke formation and contribute to deactivation [1,6,35]. During the reactions, the average carbon accumulation rate was lower and the selectivity to propene was higher for the

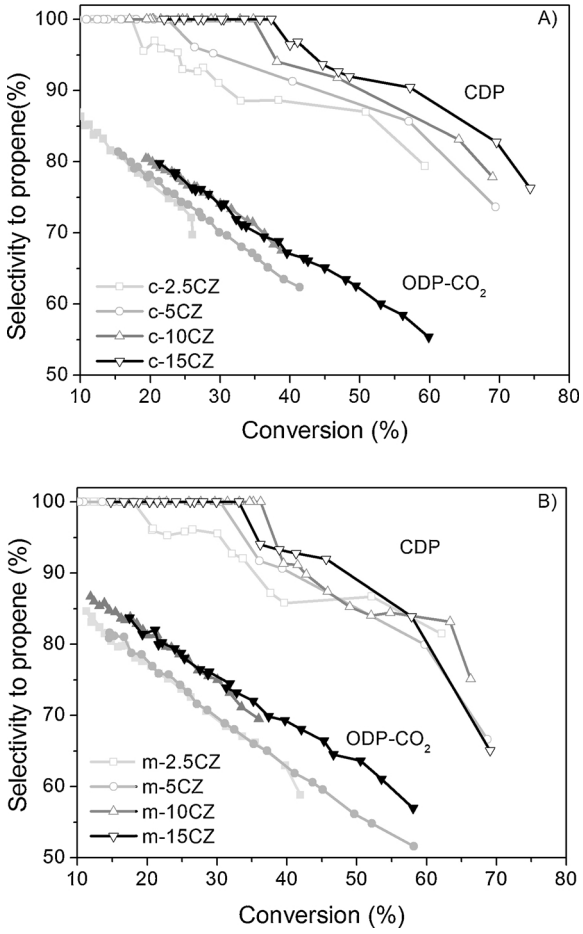

Fig. 9. Selectivity to propene as a function of propane conversion under CDP (open symbols), and ODP-CO_2 (full symbols) reaction conditions for the as-prepared x-yCZ samples (x = hydrothermal synthesis method: conventional (c-), or microwave-assisted (m-); y = Cr wt.%). GHSV was kept equal to 0.5 min, and the W/F ratio was 10 g min/L for all tests. The error of the conversion and selectivity values is estimated at about 10% of each absolute value.

catalysts with higher chromium contents (Fig. 8), while the activity decreased and the selectivity to propene increased with time on stream (Fig. 7 and 9). These results indicated that both a higher chromium oxides content and/or carbon accumulation contributed to coverage of the ZrO_2 surface and a reduction of the number of acid sites active in catalyzing the secondary reactions and decreasing the selectivity to propene.

In the ODP reaction, similarly to the behavior observed in the CDP reaction, the decrease of propane conversion was followed by increased selectivity to propene (Fig. 9A and B). Nevertheless, comparison of the data for propane conversion on stream in the CDP and ODP-CO_2 reactions (Table 3) showed that the initial propane conversion in the ODP-CO_2 reaction was strongly inhibited for some catalysts, such as conventional-yCZ (y ≤ 10 wt.%) and m-10CZ, reaching a difference of about 30% between the initial conversions. This was not observed for other catalysts such as m-15CZ and m-5CZ. Nevertheless, for the same conversion values, the selectivity to propene was always lower in the presence of CO_2 than in its absence (Fig. 9). Considering the catalysts for which propane conversion was less affected by the presence of CO_2, such as m-15CZ (Fig. 7, Table 3), the activity decreased strongly with time on stream, similarly to the CDP reaction, and the selectivity was lower in the presence of CO_2. Considering that CO_2 is a slightly acidic molecule, and that it could be adsorbed onto the basic sites of catalysts, and H_2 adsorb on the acidic sites. These results indicated that the

Table 4
Initial selectivities (S_0) towards the identified products during the CDP and ODP-CO_2 reactions for the catalysts synthesized by conventional (c-) or microwave (m) methods.

As-prepared catalyst	Reaction condition		S_0 (%)[b]					
		X_{C3H8} (%)[a]	CH_4	C_2H_4	C_2H_6	C_3H_6	C_3H_4	CO
c-5CZ	CDP	69	12 (n.d.)	2 (n.d.)	3 (n.d.)	74 (100)	1 (n.d.)	8 (n.d.)
	ODP-CO_2	41	38 (23)	n.d.	n.d.	62 (77)	n.d. (n.d.)	n.d. (n.d.)
m-5CZ	CDP	69	16 (n.d.)	2 (n.d.)	4 (n.d.)	67 (100)	2 (n.d.)	9 (n.d.)
	ODP-CO_2	58	48 (24)	n.d.	n.d.	52 (76)	n. d. (n.d.)	n. d. (n.d.)
c-15CZ	CDP	74	13 (n.d.)	1 (n.d.)	2 (n.d.)	76 (100)	1 (n.d.)	7 (n.d.)
	ODP-CO_2	59	45 (26)	n.d.	n.d.	55 (74)	n. d. (n.d.)	n. d. (n.d.)
m-15CZ	CDP	69	15 (n.d.)	1 (n.d.)	2 (n.d.)	65 (100)	3 (n.d.)	14 (n.d.)
	ODP-CO_2	58	43 (22)	n.d.	n.d.	57 (78)	n. d. (n.d.)	n. d. (n.d.)

GHSV was kept equal to 0.5 min and the W/F ratio was 10 g min/L for all tests performed at 550 °C.
The error of the data values is estimated at around 10% of each absolute value.
The values within parentheses consider the selectivities after 210 min of reaction.
Hydrogen was not detected among the products.
n.d: not detected.
[a] The initial conversion data consider a reaction time of 5 min in the CDP and ODP reactions.
[b] The initial selectivity data consider a reaction time of 5 min in the CDP and ODP reactions.

presence of CO_2 or H_2 modified the balance of acidity and basicity involved in reactions. The adsorption of CO_2 blocks the basic site involved in dehydrogenation, and favors acidity of sites that catalyzed lateral reactions, while H_2 could contribute to decrease acidity site on the ZrO_2 surface.

For CZ catalysts where the initial activity and selectivity decrease strongly with the presence of CO_2, it is reasonable to expect that CO_2 interacts with selective oxidation sites, as well as with the support surface. The negative effect of CO_2 on the activity of Cr/Al_2O_3 catalysts has been attributed to CO_2 strongly adsorbed on Al_2O_3 inhibiting the adsorption of propane [13]. Considering the catalytic results in light of the TPD-CO_2 analyses (Fig. 4), the samples that presented strong basic sites and desorption of CO_2 at high temperatures (> 500 °C), such as c-10CZ and m-10CZ, showed stronger inhibition of propane conversion due to the presence of CO_2. In order to understand these interactions of CO_2 with the ZrO_2 surface and with chromium species with different oxidation states, TPD-CO_2 experiments were performed with the reduced and as-prepared c-10CZ catalyst, comparing the results with those for the as-prepared c-Z sample (Fig. 5). Interestingly, the results revealed the presence of similar weak basic sites on the zirconia (c-Z) and the reduced c-10CZ catalysts, indicating that similar basic sites were present on the catalysts containing Cr(III) and on the zirconia surface. Nevertheless, strong basic sites of the type Cr(VI)-O-Zr were present on the as-prepared c-10CZ catalyst (Fig. 4), which adsorbed CO_2 and decomposed at high temperature. The profiles of the MS signals of O_2 (*m/z* 32) obtained during the CO_2 adsorptions are shown in Fig. 6. The results indicated that the Cr(VI) species adsorbing CO_2 could be thermally reduced at high temperature (> 500 °C). The c-10CZ and m-10CZ catalysts were those that showed the most intense CO_2 desorption but less intense O_2 formation at high temperature, while the m-15CZ catalyst showed high intensity of O_2 formation but lower intensity of CO_2 desorption at high temperature. These results indicated that CO_2 was adsorbed on basic sites such as Cr(VI)-O-Zr, and that the high lability of oxygen at the interface resulted in strong basic sites. The formation of these sites was apparently favored at a chromium content of around 10 wt.%, associated with a decrease of ZrO_2 crystallites.

The influence of strong basic sites on the performance of the catalysts in the ODP reactions seemed to be dependent on the stability of species formed by the adsorption of CO_2. For example, for the c-10CZ and m-10CZ catalysts with strong adsorption of CO_2 on chromium active sites, for which the TPD-CO_2 results indicated CO_2 desorption at temperatures of about 520 and 670 °C, respectively, the presence of CO_2 caused a strong decrease in the initial propane conversion (Fig. 7, Table 3). Interestingly, the rates of deactivation of these catalysts with time on stream (ΔX_0 ODP), shown in Table 3, were lower when compared with samples that presented low adsorption of CO_2 on strong basic sites, with desorption at high temperatures (x-yCZ catalysts with x ≤ 5 wt.% of Cr). The low deactivation of the c-10CZ and m-10CZ catalysts suggested that CO_2 adsorbed on strong basic sites participated in the catalytic cycle at high temperatures, with re-oxidation of chromium species. The reactivation of Cr(III) by CO_2 was previously reported for Cr/SiO_2 catalysts [13]. On the other hand, for the samples that showed low decreases of the initial propane conversion due to the presence of CO_2, such as the m-15CZ catalyst (Fig. 7), with desorption of CO_2 only occurring at low temperatures (Fig. 4), the intense deactivation profiles were similar to those for the CPD reaction, indicating that CO_2 did not effectively contribute to re-oxidation of the chromium species. Nonetheless, the TPR-H_2 profiles obtained after reduction and treatment with CO_2 (Table 2) demonstrated that all the Cr/ZrO_2 samples were partially re-oxidized by CO_2, even if inefficiently. This apparent disagreement with the catalytic results for samples such as m-15CZ could indicate that the reduction of Cr(VI) occurred according to the Mars-van Krevelen mechanism, with faster reduction of Cr(VI) by propane than re-oxidation of Cr(III) by CO_2.

The effectiveness of CO_2 in re-oxidation of the active sites is demonstrated in Fig. 10A and 1B, which present the propene yields of the as-prepared conventional c-5CZ catalyst in the CDP reaction, applying regeneration procedures after every 45 min on stream. In these experiments, the treatments were performed at 600 °C, using synthetic air for 5 min or pure CO_2 for 30 min. The regeneration using air resulted in the active sites being recovered over many reaction cycles. However, the effectiveness of CO_2 in catalyst regeneration decreased after two CPD reaction cycles. During the regeneration process, oxidation of carbonaceous compounds could occur via Boudouard's reaction with CO_2 or O_2 ($C + CO_{2(g)} \rightleftarrows 2CO_{(g)}$), promoting coke removal and the re-oxidation of Cr(III) to Cr(VI) species. The decreasing effectiveness of catalyst regeneration by CO_2 during the cycles suggested that the oxidation of carbonaceous compounds by CO_2 became ineffective after the first two CPD reaction cycles.

Although tuning the chromium content could promote the formation of strong basic sites such as Cr-O-Zr and result in the catalysts becoming highly stable in the presence of CO_2, the adsorption of CO_2 on the catalyst surface could lead to the catalysis of lateral reactions and strong decreases in the propene yield, as shown in Fig. 11. Further studies employing a broader set of systems are desirable in order to improve understanding of the activity and selectivity of the active sites, and their regeneration with CO_2.

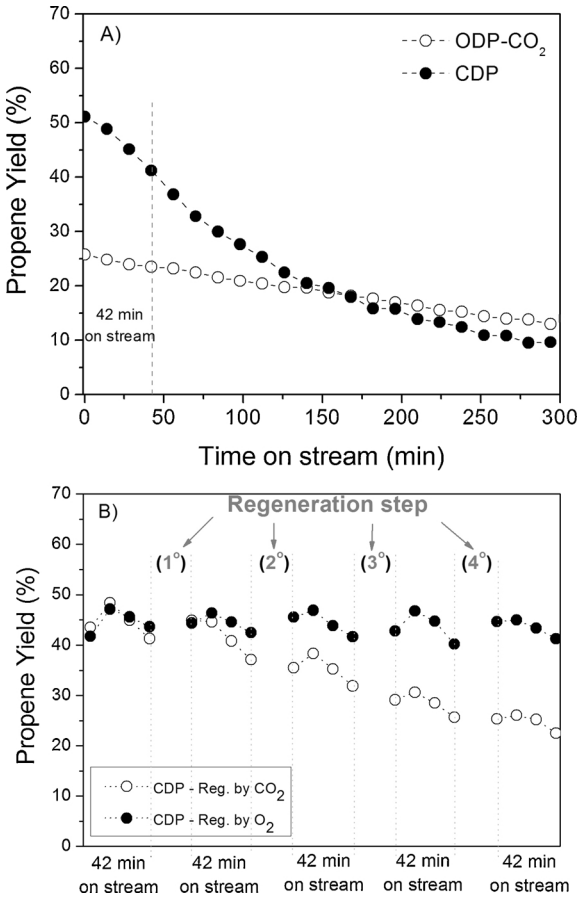

Fig. 10. Propene yields as a function of time on stream for the as-prepared c-5CZ catalyst. A: under CDP (●) and ODP-CO_2 (○) reaction conditions; B: after 300 min on stream under CDP reaction conditions with various reactivation cycles at 600 °C using O_2 for 5 min (●) and CO_2 for 30 min (○).

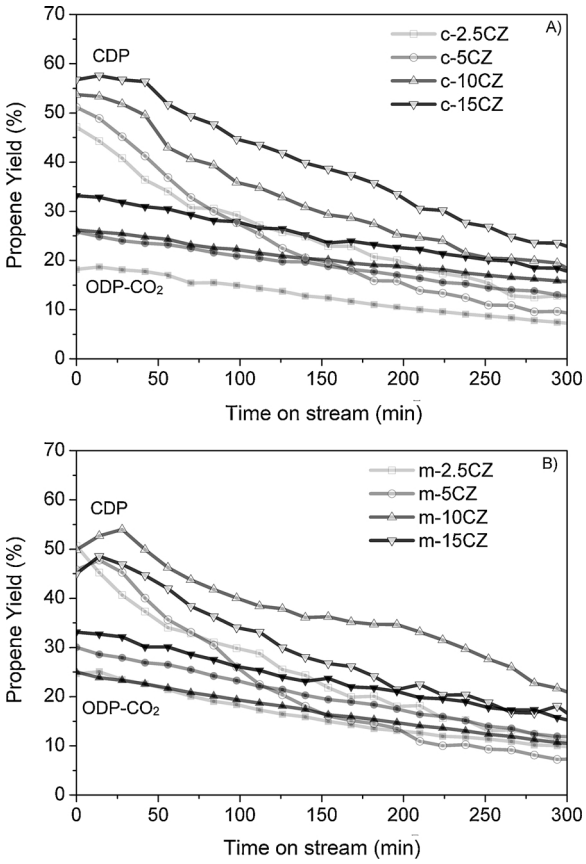

Fig. 11. Propene yields as a function of time under CDP (open symbols), and ODP-CO_2 (full symbols) reaction conditions for the as-prepared x-yCZ samples: x = hydrothermal synthesis method; A = conventional hydrothermal synthesis (c-); B = microwave-assisted hydrothermal synthesis (m-); y = Cr wt.%. GHSV was kept equal to 0.5 min and the W/F ratio was 10 g min/L for all tests.

4. Conclusions

Investigation was made of the effect of chromium content and the hydrothermal method used to prepare Cr/ZrO_2 catalysts on their catalytic properties in the dehydrogenation of propane in the presence of CO_2.

The tetragonal ZrO_2 formed showed decreasing crystallite size with increasing Cr content. The amorphous phase was obtained for samples containing Cr at ≥10 wt.%. Smaller t-ZrO_2 crystallite sizes were obtained by the microwave-assisted method.

Catalytic measurements in the presence of CO_2 indicated the existence of a relation between selectivity to propene and propane conversion, independent of the preparation method, enabling classification of the catalysts into two groups, with low (≤5%) and high (≥10%) chromium contents. The high Cr content catalysts showed higher selectivity at a given propane conversion value, indicative of similar active sites and minimization of the effects of the support on lateral reactions. The low Cr content catalysts showed higher activity, but also faster deactivation and an average rate of carbon accumulation in the presence of CO_2, especially in the case of the samples with low Cr contents obtained by the microwave-assisted method.

On the basis of the MS-assisted TPD-CO_2 results and the initial reaction rates in the presence and absence of CO_2, a fraction of the CO_2 was desorbed at temperatures higher than 500 °C, with simultaneous reduction of Cr(VI) species. The presence of CO_2 in the reactant mixture caused strong suppression of catalyst activity, selectivity, and yield towards propene. The CO_2 adsorbed strongly on the chromium oxide sites that were active and selective for the dehydrogenation of propane, enhancing the effects of the support on secondary (lateral) reactions.

In the absence of CO_2, the Cr/ZrO_2 catalysts selective for propane dehydrogenation showed deactivation rates that decreased with the chromium content, as well as increased propene yields. The results of reactivation of used catalysts with CO_2 indicated that the mechanism could not be made self-sustaining by modulating the propane and CO_2 in the feed, with the activity decreasing during sequential reaction cycles due to the deposition of carbonaceous species that could only be oxidized in the presence of O_2.

Acknowledgements

This project is supported by the Brazilian Federal Agency for Support and Evaluation of Graduate Education (CAPES) and the National Council for Scientific and Technological Development (CNPq). The authors also thank the researchers PhD. F. Rodrigues and PhD. D. Galante from University of São Paulo for Raman analysis.

Appendix A. Supplementary data

Supplementary material related to this article can be found, in the online version, at doi:https://doi.org/10.1016/j.apcata.2018.03.020.

References

[1] O.O. James, S. Mandal, N. Alele, B. Chowdhury, S. Maity, Fuel Proc. Tech. 149 (2016) 239–255.
[2] F. Cavani, N. Ballarini, A. Cericola, Catal. Today 127 (2007) 113–131.
[3] A.S. Bodke, D.A. Olschki, L.D. Schmidt, E. Ranzi, Science 285 (1999) 712–715.

[4] M.A. Atanga, F. Rezaei, A. Jawad, M. Fitch, A.A. Rownaghi, Appl. Catal. B Environ. 220 (2018) 429–445.
[5] M.S. Kumar, De Chen, J.C. Walmsley, A. Holmen, Catal. Commun. 9 (2008) 747–750.
[6] E. Daniel, E. Resasco, G.L. Haller, J.J. Spivey, S.K. Agarwal (Eds.), Catalysis, 11 Royal Society of Chemistry, Cambridge, 1994p. 379–411.
[7] C. Boucetta, M. Kacimi, A. Ensuque, J.Y. Piquemal, F. Bozon-Verduraz, M. Ziyad, Appl. Catal. A Gen. 356 (2009) 201–210.
[8] C.A. Carrero, R. Schloegl, I.E. Wachs, R. Schomaecker, ACS Catal. 4 (2014) 3357–3380.
[9] P. Mars, D.W. van Krevelen, Chem. Eng. Sci. 3 (1954) 41–57.
[10] R. Grabowski, Catal. Rev. 48 (2006) 199–268.
[11] H.H. Kung, Adv. Catal. 40 (1994) 1–38.
[12] P. Michorczyk, J. Ogonowski, P. Kústrowski, L. Chmielarz, Appl. Catal. A Gen. 349 (2008) 62–69.
[13] T. Shishido, K. Shimamura, K. Teramura, T. Tanaka, Catal. Today 185 (2012) 151–156 K.
[14] A. Pantazidis, S.A. Bucholz, H.W. Zanthoff, Y. Schuurman, C. Mirodatos, Catal. Today 40 (1998) 207–214.
[15] M.A. Bañares, Catal. Today 51 (1999) 319–348.
[16] T. Blasco, J.M. López Nieto, Appl. Catal. A Gen. 157 (1997) 117–142.
[17] S. Chen, F. Ma, A. Xu, L. Wang, F. Chen, W. Lu, Appl. Surf. Sci. 289 (2014) 316–325.
[18] A. Hakuli, A. Kyto¨ kivi, A.I. Krause, T. Suntola, J. Catal. 161 (1996) 393–400.
[19] F. Cavani, M. Koutyrev, F. Trifiro, A. Bartolini, D. Ghisletti, R. Iezzi, A. Santucci, G. Del Piero, J. Catal. 158 (1996) 236–250.
[20] K. Arata, M. Hino, H. Matsuhashi, Appl. Catal. A 100 (1993) 19–26.
[21] J.R. Sohn, S.G. Ryu, H.W. Kim, J. Mol. Catal. 135 (1998) 99–106.
[22] H. Lieske, D.L. Hoang, German patent DE-OS 196 12 000.
[23] B.M. Weckhuysen, I.E. Wachs, R.A. Schoonheydt, Chem. Rev. 96 (1996) 3327–3349.
[24] D.L. Hoang, H. Lieske, Thermochim. Acta 345 (2000) 93–99.
[25] M. Cherian, M.S. Rao, W.T. Yang, J.M. Jehng, A.M. Hirt, G. Deo, Appl. Catal. A Gen. 233 (2002) 21–33.
[26] G. Wang, L. Zhang, J. Deng, H. Dai, H. He, C.T. Au, Appl. Catal. A Gen. 355 (2009) 192–201.
[27] B.M. Weckhuysen, I.E. Wachs, J. Phys. Chem. 100 (1996) 14437–14442.
[28] M.S. Kumar, N. Hammer, M. Rønning, A. Holmen, D. Chen, J.C. Walmsley, G. Øyed, J. Catal. 261 (2009) 116–128.
[29] P. Michorczyk, J. Ogonowski, M. Niemczyk, Appl. Catal. A Gen. 374 (2010) 142–149.
[30] B.J. Xu, B. Zheng, W.M. Hua, Y.H. Yue, Z. Gao, J. Catal. 239 (2006) 470–477.
[31] M.A. Atanga, F. Rezaei, A. Jawad, M. Fitch, A.A. Rownaghi, Appl. Catal. B Env. 220 (2018) 429–445.
[32] J. Ogonowski, E. Skrzyńska, Catal. Lett. 111 (2006) 79–85.
[33] P. Michorczyk, J. Ogonowski, React. Kinet. Catal. Lett. 78 (2003) 41–47.
[34] S.B. Wang, Z.H. Zhu, Energy Fuels 18 (2004) 1126–1139.
[35] K. Takehira, Y. Ohishi, T. Shishido, T. Kawabata, K. Takaki, Q. Zhang, Y. Wang, J. Catal. 224 (2004) 404–416.
[36] R. Wu, P. Xie, Y. Cheng, Y. Yue, S. Gu, W. Yang, C. Miao, W. Hua, Z. Gao, Catal. Commun. 39 (2013) 20–23.
[37] D. Keyson, E. Longo, J.S. Vasconcelos, J.A. Varela, S. Éber, A. Der- Maderosian, Cerâmica 52 (2006) 50–56.
[38] M. Baghbanzadeh, L. Carbone, P.D. Cozzoli, C.O. Kappe, Angew. Chem. Int. Ed. Engl. 50 (2011) 11312–11359.
[39] P. Scherrer, Göttinger Nachrichten Gesell 2 (1918) 98.
[40] A. Patterson, Phys. Rev. 56 (1939) 978–982.
[41] I.C. Freitas, S. Damyanova, D.C. Oliveira, C.M.P. Marques, J.M.C. Bueno, J. Mol. Catal. A Chem. 381 (2014) 26–37.
[42] T.V.M. Rao, G. Deo, J.M. Jehng, I.E. Wachs, Langmuir 20 (2004) 7159–7165.
[43] X.Z. Zhang, Y.H. Yue, Z. Gao, Catal. Lett. 83 (2002) 19–25.
[44] D. Tuschel, Spectroscopy 31 (2016) 14–23.
[45] A.K. Arora, Rajalakshmi M, T.R. Ravindran, V. Sivasubramanian, J. Raman Spec. 38 (2007) 604–617.
[46] G. Gouadec, P. Colomban, Prog, Cryst. Growth Charact. 53 (2007) 1–56.
[47] R. Kumar, G. Sahu, S.K. Saxena, H.M. Rai, P.R. Sagdeo, Silicon 6 (2014) 117–121.
[48] I.H. Campbell, P.M. Fauchet, Solid State Commun. 58 (1986) 739–741.
[49] R. Zhang, H. Liu, D. He, Catal. Commun. 26 (2012) 244–247.
[50] A.G. Sato, D.P. Volanti, D.M. Meira, S. Damyanova, J.M.C. Bueno, J. Catal. 307 (2013) 1–17.
[51] L. Mao, B. Gao, N. Deng, L. Liu, H. Cui, Chemosphere 145 (2016) 1–9.
[52] P. Michorczyk, J. Ogonowski, K. Zenczak, J. Mol. Catal. A Chem. 349 (2011) 1–12.
[53] Y. Wang, Y. Ohishi, T. Shishido, Q. Zhang, Y. Yang, Q. Guoa, H. Wana, K. Takehira, J. Catal. 220 (2003) 347–357.
[54] A.A. Gabrienko, S.S. Arzumanov, I.B. Moroz, A.V. Toktarev, W. Wang, A.G. Stepanov, J. Phys. Chem. C 117 (2013) 7690–7702.
[55] P. Michorczyk, P. Pietrzyk, J. Ogonowski, Microporous Mesoporous Mater. 161 (2012) 56–66.
[56] T. Gott, S.T. Oyama, J. Catal. 263 (2009) 359–371.